A Fluorescence-Based Assay to Probe Inhibitory Effect of Fructose Mimics on GLUT5 Transport in Breast Cancer Cells

Natasha Rana, Marwa A. Aziz, Rabah A. T. Serya, Deena S. Lasheen, Nermin Samir, Frank Wuest, Khaled A. M. Abouzid, and F. G. West*

Read Online

ACCESS | Metrics & More | Article Recommendations | Supporting Information

ABSTRACT: Rapid cell division and reprogramming of energy metabolism are two crucial hallmarks of cancer cells. In humans, hexose trafficking into cancer cells is mainly mediated through a family of glucose transporters (GLUTs), which are facilitative transmembrane hexose transporter proteins. In several breast cancers, fructose can functionally substitute glucose as an alternative energy supply supporting rapid proliferation. GLUT5, the principal fructose transporter, is overexpressed in human breast cancer cells, providing valuable targets for breast cancer detection as well as selective targeting of anticancer drugs using structurally modified fructose mimics. Herein, a novel fluorescence assay was designed aiming to screen a series of C-3 modified 2,5-anhydromannitol (2,5-AM) compounds as D-fructose analogues

to explore GLUT5 binding site requirements. The synthesized probes were evaluated for their ability to inhibit the uptake of the fluorescently labeled D-fructose derivative 6-NBDF into EMT6 murine breast cancer cells. A few of the compounds screened demonstrated highly potent single-digit micromolar inhibition of 6-NBDF cellular uptake, which was substantially more potent than the natural substrate D-fructose, at a level of 100-fold or more. The results of this assay are consistent with those obtained from a previous study conducted for some selected compounds against ^{18}F-labeled D-fructose-based probe 6-[^{18}F]FDF, indicating the reproducibility of the current non-radiolabeled assay. These highly potent compounds assessed against 6-NBDF open avenues for the development of more potent probes targeting GLUT5-expressing cancerous cells.

KEYWORDS: GLUT5, 2,5-anhydro-D-mannitol, 6-NBDF, hydrogen bonding, structure−activity relationship
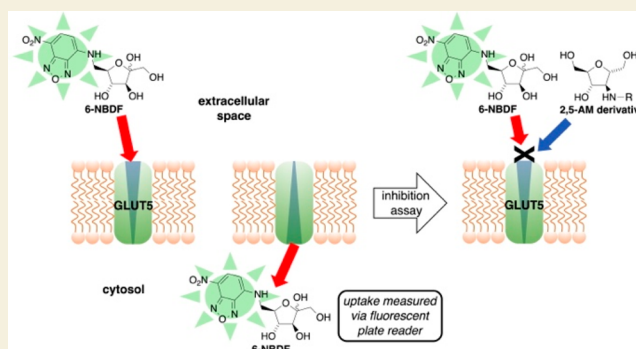
H exoses are an explicit cellular energy resource and the most essential fuel for cellular metabolism.[1] Bearing polyhydroxy substitutions, hexoses are very hydrophilic moieties that are not capable of traversing the lipid cell membrane via simple diffusion. Instead, mammalian facilitative hexose transporters (GLUTs) mediate the trafficking of hexoses from the extracellular to the intracellular space and vice versa.[2,3] GLUTs allow the passage of hexoses across the plasma membrane employing a facilitated diffusion mechanism, using existing chemical or electrochemical gradients.[2,4−6]

These GLUT proteins, encoded by the solute carrier (SLC2) genes, have been further divided into 14 known isoforms, all of which have well-established roles and a distinct pattern of tissue distribution, acting as transporters in different tissues and cell types.[7] For instance, GLUT5 is predominantly expressed in the small intestine, and one of its primary functions is mediating dietary fructose uptake across the apical membrane of the small intestine.[8] Based on amino acid sequence, substrate preferences, tissue specificity, and structural similarity, GLUTs have been classified into three major groups. Class I comprises GLUTs 1−4 and 14, which are

primarily D-glucose transporters. Class II is composed of GLUTs 5, 7, 9, and 11, among which GLUT5 shows relatively high specificity toward D-fructose. The class III family (GLUTs 6, 8, 10, 12, and 13) is structurally atypical, and its functional activity is still poorly understood.[4,7,9−12]

A wide variety of disease states, such as obesity, insulin resistance diabetes, gout, and nonalcoholic fatty liver disease, are characterized by alteration in the expression patterns of hexose transporters (GLUTs).[13−17] In addition, there is considerable interest in these GLUT transporters as a result of their overexpression in tumor cells, a phenomenon arising from altered metabolic profiles, demanding a continuous supply of hexose fuel.[17−19]

Of the 14 GLUT family members, GLUT5 shows a unique substrate preference toward D-fructose, the second most abundant energy substrate in tumor cells.[8] A metabolic switch to rely primarily upon fructose rather than glucose as the principal energy source has been detected in some cancer cells.[20] Interestingly, the high-affinity fructose transporter, GLUT5, is expressed at elevated levels in breast carcinoma cell lines,[21,22] along with numerous other cancers,[23–25] whereas its expression is limited or nonexistent in normal breast tissues.[8,21] Compared to luminal estrogen receptor-positive breast cancer, triple-negative breast cancer cells express substantially elevated levels of GLUT5 mRNA when analyzed from breast cancer patient samples.[26] Such dependence of the metabolically compromised cancerous cells on high fructose uptake provides avenues to exploit GLUT5 as a valuable target in cancer imaging and therapeutic approaches.

GLUT5, together with other GLUT transporter proteins, belongs to the larger major facilitator superfamily (MFS), having a barrel structure in which two clusters of six transmembrane helices surround the central aqueous pore containing the substrate binding site.[27–29] Recent X-ray crystal structure analyses suggest that hexose transport is achieved through a conformational shift of the protein folding between outward-open, occluded, and finally inward-open conformational states.[27–30] The presence of key hydroxyl substituents on the D-fructose scaffold, as well as their relative configuration, tends to play a fundamental role in the D-fructose–GLUT5 binding process. Furthermore, the carbon skeleton of D-fructose is reported to be responsible for the nonpolar interactions between D-fructose and hydrophobic amino acid residues of the GLUT5.[3,13,28,31]

Previously performed structure–activity relationship studies on GLUT5 demonstrated the ability of its binding pocket to accept D-fructose in its furanose and pyranose ring forms.[32] Moreover, the C-1, C-3 and C-4 hydroxyl groups of D-fructose appear to form essential hydrogen bonding interactions with specific amino acid residues within the binding pocket for efficient uptake.[13,32,33] In contrast, the hydroxyl groups at C-2 and C-6 were found to play a negligible role in substrate recognition, rendering several C-2 and C-6 labeled D-fructose analogues readily handled by GLUT5.[13,32–35] However, in the case of C-6-modified fructose analogues, accumulation after GLUT5-mediated uptake is hampered due to the absence of the C-6 alcohol that is ordinarily phosphorylated by hexokinase. Without the introduction of the negatively charged phosphate group, efflux can occur, leading to eventual depletion of the probe concentration within the cell.[36,37]

The absence of the C-2 hemiacetal hydroxyl group of D-fructose affords the C_2-symmetric derivative 2,5-anhydro-D-mannitol (2,5-AM), which exhibits a slightly higher affinity to GLUT5 (K_i = 12.6 mM) than D-fructose (K_i = 16 mM).[32] 2,5-AM is permanently locked in a furanose form due to the absence of a hemiacetal at C-2, rendering C-1 and C-6 hydroxyl groups equal and susceptible to hexokinase or ketohexokinase (fructokinase) phosphorylation. To mitigate the tendency to undergo efflux observed with C-6 modified D-fructose analogues, the two primary hydroxyl groups at C-1/C-6 of 2,5-AM should be left intact, while modifications at C-3 or C-4 positions could be evaluated and optimized for their tolerability by GLUT5.

We have previously described an examination of a series of C-3 modified 2,5-AM derivatives, with a focus upon hydrogen bond donor/acceptor properties of the C-3 substituents for

their ability to inhibit the uptake of [^{14}C]-D-fructose into GLUT5-expressing EMT6 murine mammary carcinoma cells. This study found that retention of hydrogen bond donor capacity at C-3 is critical for high-affinity binding to GLUT5 and uptake into cells.[38] In a further complementary study aiming to provide more broad insight into GLUT5 structural demands and binding pocket requirements, a selection of C-3 modified 2,5-AM probes possessing different hydrogen bond donor moieties and steric demand were synthesized.[39] The transport properties of these probes were investigated in EMT6 breast cancer cell lines against the radiolabeled GLUT5 substrate [^{18}F]-6-deoxy-6-fluoro-D-fructose (6-[^{18}F]FDF), using the non-radiolabeled fructose derivative, 6-FDF **1** (Figure 1), as the reference compound (IC$_{50}$ = 19 mM).[35,37]
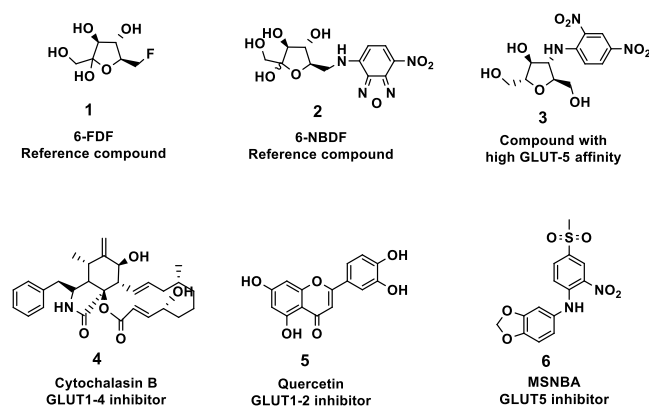
Figure 1. Reference compounds with known affinities for various GLUTs.

Relative to 6-FDF, several compounds displayed stronger inhibitory activity on 6-[^{18}F]FDF uptake into EMT6 cells, at 5–15-fold levels.[39] Figure 1 presents reported analogues and inhibitors acting through different GLUT pathways.[31,35,38,40–45]

In the current study, a fluorescent-based assay has been developed with the ultimate purpose of evaluating the affinity of various C-3 modified 2,5-AM compounds to GLUT5 protein, using our own synthesized reference compound, 6-NBDF, **2** (6-NBD-D-fructose; NBD = 7-nitrobenz-2-oxa-1,3-diazolyl). This fluorescently labeled fructose analogue is exploited as an alternative reference compound to 6-[^{18}F]FDF, eliminating any need for radiochemical synthesis and relying on a readily available fluorescent plate reader for measurement of uptake (Figure 1). With this probe in hand, we designed and synthesized a library of C-3 modified 2,5-AM derivatives bearing a range of hydrogen bond donor functionalities (anilines, amides, sulfonamides, ureas, and thioureas). Along with several previously reported 2,5-AM derivatives,[39] this set of compounds was then assessed in EMT6 murine mammary carcinoma cells using a fluorescence-based assay to detect inhibition of GLUT5-mediated uptake (Figure 2). In addition, we also performed this assay with known GLUT inhibitors **3**–**6** (Figure 1) that could function as positive controls. This study was pursued with the goal of identifying GLUT5 binding pocket requirements by evaluating our library of C-3 modified 2,5-AM derivatives through the newly designed fluorescence-based assay against 6-NBDF. The results of these evaluations could then be exploited for the design and development of high-affinity GLUT5-selective
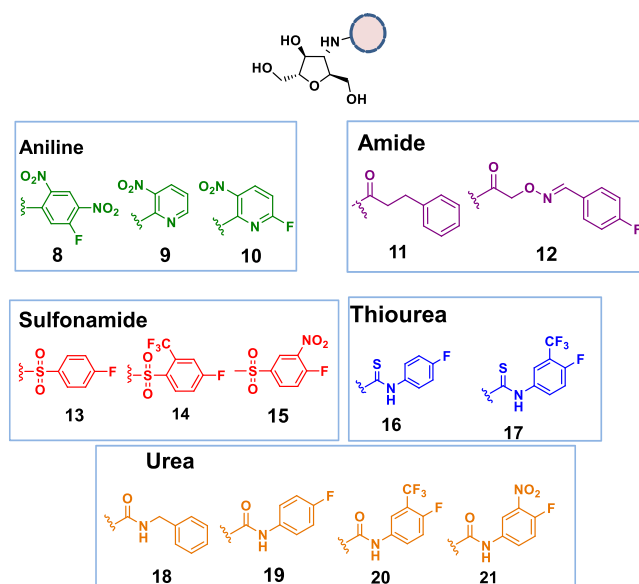
Figure 2. C-3 modified 2,5-AM derivatives evaluated in our fluorescence-based assay.

compounds for use in molecular imaging or therapeutic applications.

RESULTS AND DISCUSSION

Synthesis

Various C-3 modified 2,5-AM compounds **9**, **10**, **11**, **15**, **17**, **18**, **19**, **20**, and **21** were synthesized according to the synthetic route depicted in Scheme 1, while compounds **8**, **12**, **13**, **14**, and **16** were synthesized according to the previously reported procedure.[39] The key intermediate 3-amino-3-deoxy-2,5-anhydro-D-mannitol **7** was prepared according to the published procedure[46] and was then functionalized to different C-3 modified 2,5-AM derivatives. The pyridylamino derivatives **9** and **10** herein were obtained through reacting amine **7** with 2-chloro-3-nitropyridine and 2,6-difluoro-3-nitropyridine, respectively, in DMF, via nucleophilic aromatic substitution (S_NAr) at the nitro-activated fluorinated positions. In the case of **10**, regioselectivity was observed as the amino group of 3-amino-3-deoxy-2,5-AM displaced the 2-fluoro group of the pyridine reagent exclusively. The synthesis of the amide derivative **11** was accomplished by treating amine **7** with N-hydroxy-succinimidyl dihydrocinnamate[47] in methanol. Regarding sulfonamide derivative **15**, its preparation involved a condensation reaction between amine **7** and 4-fluoro-3-nitrobenzenesulfonyl chloride[48] in the presence of sodium carbonate and acetonitrile at ambient temperature. To afford thiourea compound **17**, amine **7** was reacted with 4-fluorophenyl-3-(trifluoromethyl)phenyl isothiocyanate in methanol for 15 h. Finally, **7** was treated with different isocyanate derivatives in DMF at room temperature, affording the urea derivatives **18−21** in good yields.

Biological Evaluation

Validation of 6-NBDF as a Reference Compound. 6-NBDF probe **2**, the reference compound used in the assay under development, has been previously proven to be selectively transported via the GLUT5 pathway and could have the potential to serve as a laboratory tool for assessing the trafficking of D-fructose mimics inside GLUT5-expressing

Scheme 1. Synthesis of C-3 Modified 2,5-AM Derivatives
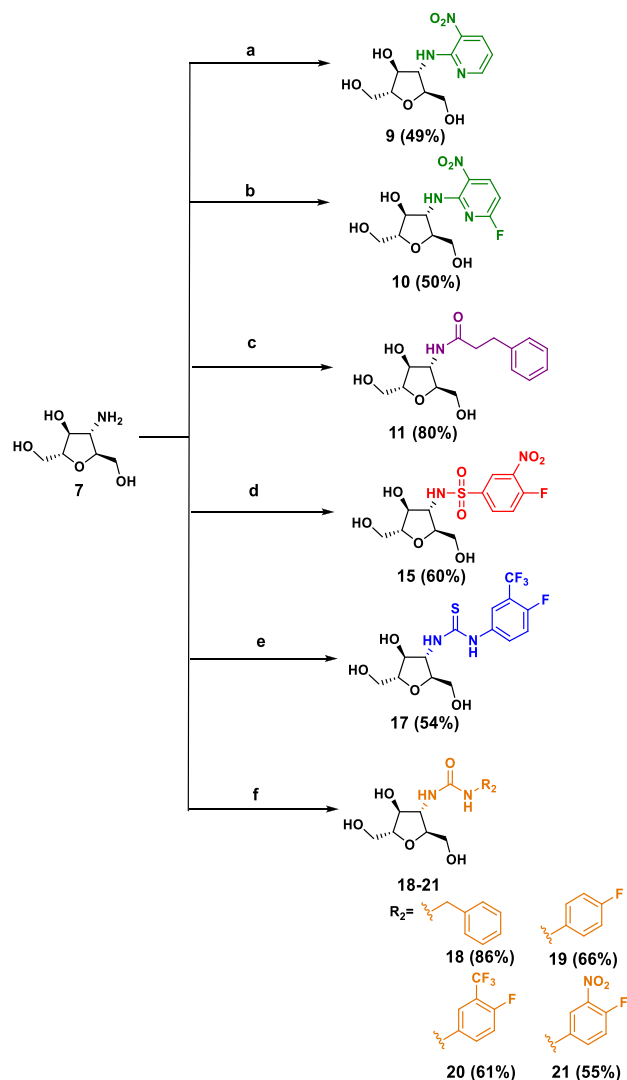
[a]Reagents and conditions: (a) 2-chloro-3-nitropyridine, NaHCO₃, DMF, rt, 12 h then 80 °C, 15 h, 47%; (b) 2,6-difluoro-3-nitropyridine, NaHCO₃, DMF, rt, 2 h, 50%; (c) N-hydroxy-succinimidyl dihydrocinnamate, MeOH, rt, 2 h, 80%; (d) 4-fluoro-3-nitro-benzenesulfonyl chloride, Na₂CO₃, MeCN, rt, 16 h, 60%; (e) 4-fluorophenyl-3-(trifluoromethyl)phenyl isothiocyanate, MeOH, rt, 15 h, 54%; (f) isocyanate derivatives (benzyl isocyanate, 4-fluorophenyl isocyanate, 4-fluoro-3-(trifluoromethyl)phenyl isocyanate, or 4-fluoro-3-nitrophenyl isocyanate), DMF, rt, 15 h.

breast cancer cells.[31] 6-NBDF was taken up rapidly into the mammalian EMT6 cell line mainly via GLUT5 machinery and competitively inhibited the uptake of [¹⁴C]-D-fructose, the natural substrate of GLUT5 enzyme, with IC₅₀ = 2.9 ± 1.14 mM.[31] In addition, complementary qualitative confocal microscopy experiments were conducted, offering compelling evidence for 6-NBDF cell internalization. Furthermore, the uptake was inhibited in the presence of D-fructose but was unaffected by D-glucose, indicating its primary uptake via GLUT5 rather than the high-affinity glucose transporter, GLUT2.[31] These studies provided key support for the hypothesis that 6-NBDF (**2**) could serve as a reference compound in our proposed fluorescence-based GLUT5 assay.

To evaluate the suitability of **2**, as a reference compound in this inhibition assay, several preliminary experiments were

conducted. First, concentration-dependent uptake of **2** by EMT6 cancer cell lines was examined. A linear relationship of fluorescence intensity occurred with the incubation of EMT6 cells with increasing concentrations of probe **2** (Figure 3A).
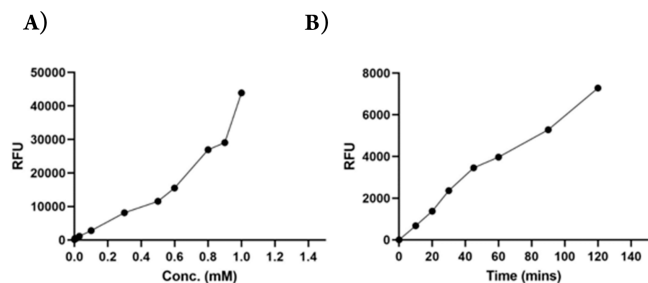
Figure 3. (A) Concentration-dependent uptake of 6-NBDF into EMT6 cells with different concentrations ranging from 10^{-7} to 10^{-3} M. (B) Time-dependent uptake of 350 μM 6-NBDF into EMT6 cells measured at different time intervals up to 2 h.

Second, 350 μM **2** was incubated in EMT6 cells at different time intervals over a 2 h period to determine the time-dependent uptake of the probe compound. As anticipated, the fluorescence signal was detected to be continuously increasing with time (Figure 3B). An increase in fluorescence intensity in both concentration and time-based manner would establish the basis for optimization of an inhibition assay to determine the optimal time and concentration of 6-NBDF to be used for further steps.

In Vitro 6-NBDF Uptake Inhibition Assay with C-3 Modified 2,5-AM Compounds. The impact of structural variation among the novel C-3 modified 2,5-AM compounds described above was investigated to gain a better understanding of the interactions required for GLUT5 recognition. The murine mammary carcinoma cell line EMT6 was used in these experiments to measure the concentration-dependent inhibition of their uptake of 6-NBFD (**2**) by derivatives **8−21**. The concentration-dependent inhibition of 6-NBDF uptake into EMT6 cells in the presence of compounds **8−21** and their IC$_{50}$ values are depicted in Table 1 and Figure 4.

We initiated our study by investigating the effect of D-fructose as a positive control to study its inhibitory effect on 6-NBDF uptake. An IC$_{50}$ of 1.7 M was observed, which is quite high even though D-fructose is the natural substrate of GLUT5 (Table 1 and Figure 4).

Aniline derivatives **8**, **9**, and **10**, were all shown to be potent inhibitors of 6-NBDF uptake into EMT6 cells compared to D-fructose, with IC$_{50}$ values of 1.05, 2.24, and 0.99 mM respectively. These findings are consistent with our previously reported results with compound **8**, which was found to be a potent inhibitor of 6-[^{18}F]FDF uptake into the EMT6 cell line (Table 1 and Figure 4A).[39] Such potent activity exerted by these probes may be attributed to the collective electron-withdrawing effect of the aryl substituents on the aniline nitrogen atom, rendering it a more effective hydrogen bond donor.

Moving to the amide-bearing derivatives, compound **11** exhibited no effect on 6-NBDF uptake into EMT6 cells. However, compound **12**, with an aryl ring incorporated by a slightly longer tether compared to **11**, displayed significant inhibitory activity with IC$_{50}$ = 1.48 mM, demonstrating the affinity and tolerability of the GLUT5 binding pocket to oxime ether linkage on the tether. Again, some consistency was

Table 1. Half-Maximum Inhibition Concentrations (IC$_{50}$) for C-3 Modified 2,5-AM Compounds 8−21, D-Fructose, GLUT Substrate 3, Cytochalasin B (4), Quercetin (5), and MSNBA (6) against the Uptake of 6-NBDF into EMT6 Cells

| compound	IC$_{50}$ (mM) against 6-NBDF	IC$_{50}$ (mM) against 6-[^{18}F]FDF[a]
8	1.05	1.10 ± 0.17
9	2.24	c
10	0.99	c
11	b	c
12	1.48	2.31 ± 0.35
13	b	~6[d]
14	4.63	b
15	1.61	c
16	b	b
17	6.84	c
18	2.16	c
19	13.25	c
20	2.88	c
21	5.04	c
compound 3	2.92	c
cytochalasin B	b	e
quercetin	b	c
MSNBA	b	b
D-fructose	1710	342 ± 74

[a]For comparison, previously reported IC$_{50}$ values for compounds **8**, **12**, **13**, **14**, and **16** against the uptake of 6-[^{18}F]FDF[39] into EMT6 cells are also shown. Data are shown as mean ± SEM from 9 data points out of 3 experiments (n/x = 9/3) [b]Not determined. [c]Not performed. [d]Estimated. [e]50% inhibition was observed.

noticed with our previous 6-[^{18}F]FDF uptake result, where **12** showed potency in inhibiting the uptake of 6-[^{18}F]FDF with an IC$_{50}$ of 2.31 ± 0.35 mM[39] (Table 1 and Figure 4B).

Regarding compounds **13**, **14**, and **15**, bearing sulfonamide handles, it is noted that **13** displayed no inhibition of uptake of 6-NBDF by EMT6 cells. Interestingly, sulfonamides **14** and **15** showed strong inhibitory potency with IC$_{50}$ values of 4.63 and 1.61 mM, respectively. In contrast, sulfonamide **13** did moderately inhibit the uptake of 6-[^{18}F]FDF with an approximate IC$_{50}$ of 6 mM[39] (Table 1 and Figure 4C). For compounds **14** and **15**, the mentioned observations could be delineated due to the presence of electron-withdrawing aryl substituents ($-CF_3$ and $-NO_2$), which serve to elevate the hydrogen donor capability of the sulfonamide NH linker, with a nitro group being a stronger electron-withdrawing moiety than the trifluoromethyl group.

Thiourea **16** displayed no inhibitory effect on 6-NBDF uptake, in agreement with earlier results obtained using 6-[^{18}F]FDF.[39] However, compound **17** displayed relatively weak inhibition with an IC$_{50}$ of 6.84 mM (Table 1 and Figure 4D).

Finally, upon evaluating the novel urea-linked 2,5-AM derivatives **18−21**, it was observed that urea functionalization at C-3 in compounds **18**, **20**, and **21** is generally tolerated and resulted in a significant increase in the inhibition efficacy in comparison to D-fructose, with IC$_{50}$ values of 2.16, 2.35, and 5.04 mM, respectively. However, compound **19**, bearing a *para*-fluoro substituent on the terminal phenyl group, exhibited a relatively higher IC$_{50}$ value of 13.25 mM (Table 1 and Figure 4E). In the case of urea- and thiourea-containing derivatives, substituents on the benzyl ring are not involved in conjugation with NH at C-3, and the presence of these substituents on the aryl ring would not participate in influencing the hydrogen
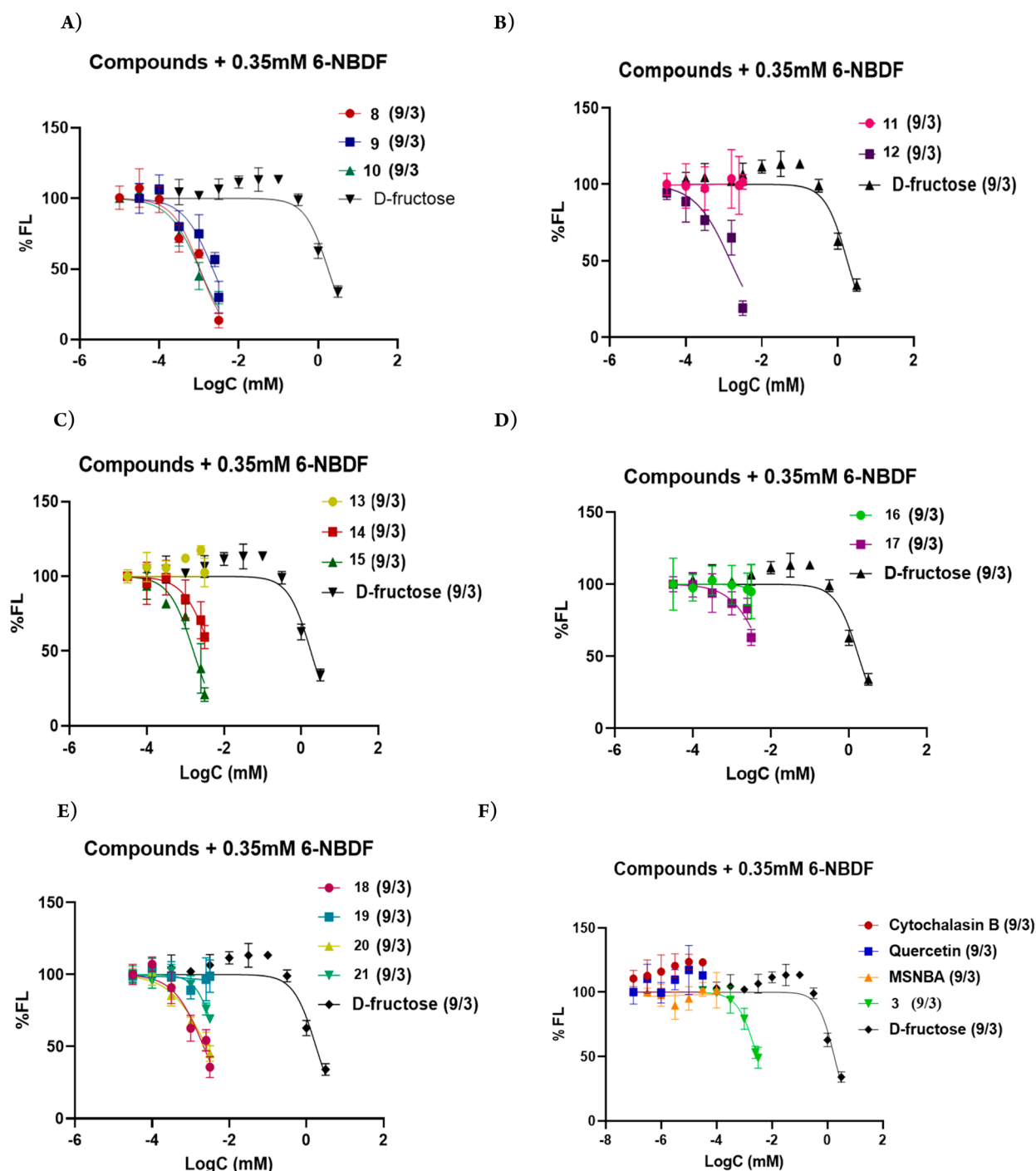
Figure 4. Concentration-dependent inhibition of 6-NBDF uptake into EMT6 cells of C-3 modified 2,5-AM compounds. (A) Compounds **8−10** and D-fructose. (B) Compounds **11**, **12**, and D-fructose. (C) Compounds **13−15** and D-fructose. (D) Compounds **16**, **17**, and D-fructose. (E) Compounds **18−21** and D-fructose. (F) GLUT5 substrate **3**, cytochalasin B (**4**), quercetin (**5**), MSNBA (**6**), and D-fructose. Data are shown as mean ± SEM of 9 data points from 3 experiments.

bonding capacity of NH at C-3. Compound **20**, bearing the para fluorine and meta trifluoromethyl substituent, similar to that of thiourea derivative **17**, exhibited similar potency with a slight difference in IC_{50} values (6.84 vs 2.88 mM). This might suggest a similar type of binding interactions of these two compounds with GLUT5. Lastly, compound **21** demonstrated a moderate inhibitory activity with an IC_{50} of 5.04 mM. Overall, the variations seen among the individual members of this small screening library suggest that additional interactions

beyond those identified previously[39] are at play in the GLUT5 binding pocket.

Furthermore, we examined the 6-NBDF uptake profile in the presence of different GLUT inhibitors. Cytochalasin B (**4**), an established inhibitor of GLUT1−4 facilitated transport,[40,41] as well as quercetin (**5**), which competitively inhibits glucose entry via GLUT1−2,[42,43] afforded no decrease in the uptake of 6-NBDF by EMT6 cells (Table 1 and Figure 4F). The absence of any apparent effects by known class I GLUT inhibitors provides good evidence that uptake of 6-NBDF (**2**) occurs via

the principal fructose transporter, GLUT5. In addition, the effect of N-[4-(methylsulfonyl)-2-nitrophenyl]-1,3-benzodioxol-5-amine (MSNBA, 6) was also studied against 6-NBDF entry into the EMT6 cancer cell line. 6 is the first reported selective inhibitor of GLUT5, with an IC_{50} value of 5.8 ± 0.5 μM and was used to test the inhibition of yeast-expressed GLUT5.[44,45] Surprisingly, no drop in 6-NBDF uptake was observed in the presence of 6 due to its limited water solubility, which prevented its use at concentration greater than 0.1 mM (Table 1 and Figure 4F).

Moreover, compound 3, which was previously shown to be a potent inhibitor of [^{14}C]-D-fructose uptake,[39] was also investigated against the uptake of 6-NBDF (2). Predictably, it was found to strongly inhibit 6-NBDF uptake with an IC_{50} of 2.92 mM (Table 1 and Figure 4F). Confirmation of inhibition of uptake of 2 by reference compound 3 but not by 4 or 5 confirms that this assay can detect novel inhibitors of GLUT5 uptake, as seen with several of the 2,5-AM derivatives.

In light of these results, the GLUT5 inhibitory activity of the newly screened 2,5-AM derivatives confirms the importance of a C-3 hydrogen bond donor and the significance of linkers and steric demand. Out of the different functional group linkers tested, compounds having electron deficient aniline displayed maximum potency followed by compounds having sulfonamide linkers. In addition, some compounds gave contradictory results in this assay and the previously reported one that relied on 6-[^{18}F]FDF as the reference compound. The differences seen in the IC_{50} values for the two reference compounds may derive from additional binding interactions available to 6-NBDF via the large, nonpolar fluorophore attached at C-6. In addition, while uptake of 6-NBDF is mediated primarily by GLUT5,[31] there is evidence that 6-[^{18}F]FDF is taken up via both GLUT5 and GLUT2.[49] Compound 14 displayed inhibition of 6-NBDF uptake, whereas no inhibition was observed in 6-[^{18}F]FDF uptake. This might suggest that a higher concentration of this compound is needed to cause inhibition of 6-[^{18}F]FDF uptake and it is more selective to GLUT5 causing strong inhibition in fluorescence of 6-NBDF. In contrast, in the case of compound 13, inhibition in the uptake of 6-[^{18}F]FDF was observed with no inhibition observed in the uptake of 6-NBDF. Exclusive inhibition of 6-[^{18}F]FDF uptake but not 6-NBDF suggests that 13 may interact primarily with GLUT2 rather than GLUT5. Regarding different GLUT inhibitors tested, none of the inhibitors caused any measurable inhibition of 6-NBDF uptake. Surprisingly, the previously reported GLUT5 inhibitor MSNBA did not show even slight inhibition at the concentration reported at which it exerts 50% inhibition in D-[^{14}C]-fructose uptake. Further studies will be needed to understand the reasons for this lack of inhibition.

CONCLUSION

In summary, we have shown that 6-NBDF can be used as a reference standard to screen for inhibition of fructose mimic transport by GLUT5 using fluorescence measurements. We also observed that inhibition values were in the same range for compounds tested in the 6-[^{18}F]FDF inhibition assay, with the exception of D-fructose and compounds 13 and 14. Relative performance by 6-NBDF compared to the earlier radiolabeled probe 6-[^{18}F]FDF raises the possibility of easy generalization and automation of the assay, potentially allowing for a high-throughput screen of large libraries to identify novel GLUT5 inhibitors.[50] Along with this newly developed fluorescent assay,

14 novel and previously reported C-3 modified 2,5-AM compounds were characterized for their ability to inhibit the uptake of 6-NBDF, which is taken to be a surrogate for their GLUT5 affinity. Among the synthesized compounds in this library, 11 compounds displayed much higher potency than the natural ligand for GLUT5, D-fructose. In addition, it was observed that D-fructose displayed an IC_{50} of 1.7 M, which is 5-fold higher than the IC_{50} value observed in the 6-[^{18}F]FDF inhibition assay (322 mM). This observation suggests that GLUT5 may display greater affinity for 6-NBDF than for 6-[^{18}F]FDF. Future studies are needed to understand the binding kinetics as well as the type of inhibition (competitive, allosteric, uncompetitive) exhibited by these compounds. Such studies can be accomplished by performing a "saturation" binding experiment with a cell line containing a single expression system of transporter protein alone (GLUT5) that would help in determining K_i or K_D for each derivative. Our "competitive" binding experiment in a cell-based system using 6-NBDF for competition only allows for a relative comparison between different compounds by determining the "potency" with IC_{50} values in EMT6 cancer cells expressing different GLUTs. Studies by Chen et al. have noted synergy in the elimination of acute myeloid leukemia cells between 2,5-AM and a cell-cycle inhibitor, arabinofuranosylcytidine.[25] The C3-modified 2,5-AM derivatives reported here may serve as starting points for the development of potential therapeutic agents. Furthermore, since elevated expression of GLUT5 is associated with other disease states besides breast cancer, these compounds could serve in other imaging and therapeutic applications.

■ EXPERIMENTAL SECTION

Synthetic Chemistry and Analysis

Reactions were carried out in oven-dried glassware under a positive argon or nitrogen atmosphere unless otherwise stated. Transfer of anhydrous solvents and reagents was accomplished with oven-dried syringes or cannulae. Solvents were obtained from a solvent purification system. Thin layer chromatography was performed on glass plates preloaded with 0.25 mm silica gel matrix, mixed with F_{254} fluorescent indicator. Flash chromatography columns were packed with 230−400 mesh silica gel. Optical rotations were measured at 22 ± 2 °C. Proton nuclear magnetic resonance spectra (^{1}H NMR) were recorded at 400, 600, or 700 MHz, and coupling constants (J) are reported in Hertz (Hz). Standard notation was used to describe the multiplicity of signals observed in ^{1}H NMR spectra: broad (br), multiplet (m), singlet (s), doublet (d), triplet (t), etc. Carbon nuclear magnetic resonance spectra (^{13}C NMR) were recorded at 125 MHz and are reported as δ (ppm) relative to the center line of the septet from methanol-d_4 (49.3 ppm), the triplet of chloroform-d (77.2 ppm), or the septet of DMSO-d_6 (39.5 ppm). Mass spectra were determined on a high-resolution electrospray spectrometer. Purity of probe compounds was measured via HPLC (C18, 4.6 mm × 250 mm, 0.6 mL/min; gradient elution solvent A, 0.1% TFA in water; gradient elution solvent B, 0.1% TFA in acetonitrile).

Synthesis

C-3 modified 2,5-AM compounds 8, 12, 13, 14, and 16 were synthesized according to their reported procedures.[39] GLUT inhibitors cytochalasin B (4) and quercetin (5) were purchased from Sigma−Aldrich Inc. GLUT5 inhibitor MSNBA (6) was synthesized following the reported procedure.[49] Key amine compound 3-amino-3-deoxy-2,5-anhydro-D-mannitol (7) was prepared from 3-azido-3-deoxy-2,5-anhydro-D-mannitol according to the reported procedure.[46] N-Hydroxy-succinimidyl dihydrocinnamate and 4-fluoro-3-nitrobenzenesulfonyl chloride were synthesized following their reported procedures.[47,48]

3-Deoxy-3-[*N*-(3-nitropyridin-2-yl)amino]-2,5-anhydro-D-mannitol (9). Amine **7** (0.12 g, 0.73 mmol) was stirred in dry DMF (12 mL) in a 1-neck round-bottom flask under N_2 atmosphere until it was completely dissolved. An excess of $NaHCO_3$ (0.49 g, 5.8 mmol) was added to the flask, followed by the addition of 2-chloro-3-nitropyridine (0.24 g, 1.4 mmol). The reaction mixture was stirred at room temperature for 12 h, then heated to 80 °C and stirred for an additional 15 h. The reaction mixture was allowed to cool to room temperature, and solids were removed by filtration. The filtrate was concentrated under reduced pressure, and the resulting crude product was subjected to silica gel column chromatography and eluted with a DCM/MeOH solvent mixture (gradient from 100:0 to 95:5). Fractions containing the desired product were combined and concentrated under vacuum providing **9** as a yellow sticky solid (0.11 g, 49%). R_f 0.40 (DCM/MeOH, 90:10); $[\alpha]_D^{20} = -2.94$ (*c* 0.17, MeOH); FT-IR (cast film) 3341, 2956, 2920, 2851, 2102, 1733, 1609, 1508, 1444, 1411, 1377, 1358, 1314 cm^{-1}. ^{1}H NMR (700 MHz, CD$_3$OD): δ 8.49 (dd, *J* = 8.3, 1.8 Hz, 1H), 8.44 (dd, *J* = 4.5, 1.8 Hz, 1H), 6.79 (dd, *J* = 8.3, 4.5 Hz, 1H), 4.76 (t, *J* = 6.0 Hz, 1H), 4.26 (t, *J* = 5.8 Hz, 1H), 4.04 (ddd, *J* = 6.4, 5.5, 3.6 Hz, 1H), 3.98 (ddd, *J* = 5.9, 4.4, 2.8 Hz, 1H), 3.79 (dd, *J* = 5.5, 3.3 Hz, 1H), 3.78 (dd, *J* = 5.6, 3.2 Hz, 1H), 3.74 (dd, *J* = 12.0, 5.5 Hz, 1H), 3.69 (dd, *J* = 11.9, 4.4 Hz, 1H), 4 exchangeable protons were not detected in CD$_3$OD solution. ^{13}C NMR (176 MHz, CD$_3$OD): δ 156.3, 153.6, 136.5, 130.0, 113.5, 86.1, 85.2, 78.2, 63.8, 63.2, 61.3. HRMS (ESI) calcd for C$_{11}$H$_{14}$N$_3$O$_6$ [M − H]$^-$ 284.0888; found 284.0895. HPLC purity >96%.

3-Deoxy-3-[*N*-(6-fluoro-3-nitropyridin-2-yl)amino]-2,5-anhydro-D-mannitol (10). Amine **7** (0.14 g, 0.86 mmol) was stirred in freshly distilled DMF (20 mL) under N_2 atmosphere until it was completely dissolved. An excess of $NaHCO_3$ (0.57 g, 6.8 mmol) and 2,6-difluoro-3-nitropyridine[51,52] (0.14 g, 0.86 mmol) was subsequently added, and vigorous stirring was continued at room temperature for 2 h. Solids were removed by filtration before the resultant filtrate was concentrated under reduced pressure. The obtained crude compound was purified via silica gel column chromatography using a DCM/MeOH solvent mixture (gradient from 100:0 to 95:5). Fractions containing the desired product were combined and concentrated under vacuum to yield **10** as a yellow solid (0.13 g, 50%). R_f 0.3 (DCM/MeOH, 90:10); $[\alpha]_D^{20} = -1.06$ (*c* 0.17, MeOH); FT-IR (cast film) 3327, 2951, 2919, 2851, 1624, 1582, 1544, 1458, 1432, 1362, 1331, 1259 cm^{-1}. ^{1}H NMR (400 MHz, CD$_3$OD): δ 8.62 (dd, *J* = 8.9, 7.0 Hz, 1H), 6.36 (dd, *J* = 8.9, 3.2 Hz, 1H), 4.69 (t, *J* = 5.4 Hz, 1H), 4.27 (t, *J* = 5.3 Hz, 1H), 4.04 (td, *J* = 5.6, 3.8 Hz, 1H), 3.98 (ddd, *J* = 5.5, 4.0, 2.7 Hz, 1H), 3.80−3.75 (m, 2H), 3.68 (dd, *J* = 11.9, 4.0 Hz, 1H), 3.62 (dd, *J* = 7.9, 5.5 Hz, 1H), 4 exchangeable protons were not detected in CD$_3$OD solution. ^{13}C NMR (176 MHz, D$_2$O): δ 164.1 (d, J_{C-F} = 375.1 Hz), 153.4, 143.1 (d, J_{C-F} = 12.6 Hz), 126.9, 99.3 (d, J_{C-F} = 40.3 Hz), 84.2, 82.9, 76.5, 62.2, 62.1, 59.2. HRMS (ESI) calcd for C$_{11}$H$_{13}$FN$_3$O$_6$ [M − H]$^-$ 302.0794; found 302.0787. HPLC purity >99%.

3-Deoxy-3-[*N*-dihydrocinnamido]-2,5-anhydro-D-mannitol (11). Amine **7** (0.25 g, 1.5 mmol) was dissolved in MeOH (5 mL) under N_2 atmosphere. To the homogeneous mixture, *N*-hydroxysuccinimidyl dihydrocinnamate[47] (0.38 g, 1.5 mmol) was added, and the mixture was stirred for 24 h at room temperature. The reaction mixture was concentrated under reduced pressure. The obtained crude compound was purified via silica gel column chromatography using a DCM/MeOH solvent mixture (gradient from 100:0 to 95:5). Fractions containing the desired product were combined and concentrated under vacuum to obtain **11** as a yellow sticky solid (0.37 g, 80%). R_f 0.5 (DCM/MeOH, 90:10); $[\alpha]_D^{20} = 5.00$ (*c* 0.10, MeOH); IR (cast film) 3278, 3064, 2920, 2852, 2919, 1649, 1557, 1453, 1378, 1323, 1050, 718 cm^{-1}. ^{1}H NMR (400 MHz, CD$_3$OD): δ 7.26 (t, *J* = 7.6 Hz, 2H), 7.22−7.19 (m, 2H), 7.18−7.15 (m, 1H), 4.14 (t, *J* = 7.4 Hz, 1H), 3.99 (t, *J* = 7.0 Hz, 1H), 3.81 (ddd, *J* = 7.3, 5.0, 3.0 Hz, 1H), 3.70 (dd, *J* = 12.0, 3.0 Hz, 1H), 3.66 (ddd, *J* = 7.6, 5.6, 3.1 Hz, 1H), 3.62−3.58 (m, 1H), 3.58−3.55 (m, 1H), 3.51 (dd, *J* = 12.0, 5.6 Hz, 1H), 2.91 (dd, *J* = 15.7, 8.0 Hz, 2H), 2.51 (td, *J* = 7.5, 4.3 Hz, 2H), 4 exchangeable protons were not detected in CD$_3$OD solution. ^{13}C NMR (176 MHz, CD$_3$OD): δ 174.3, 140.6, 128.05,

128.01, 125.8, 83.6, 82.0, 75.2, 62.2, 61.4, 57.7, 37.4, 31.4. HRMS (ESI) calcd for C$_{15}$H$_{21}$NNaO$_5$ [M + Na]$^+$ 318.1308; found 318.1312. HPLC purity >95%.

3-Deoxy-3-[*N*-4-fluoro-3-nitro-benzenesulfonamido]-2,5-anhydro-D-mannitol (15). A 50 mL round-bottomed flask, maintained under N_2 atmosphere, was charged with amine **7** (0.22 g, 1.3 mmol), which was dissolved in freshly distilled MeCN (15 mL). 4-Fluoro-3-nitrobenzenesulfonyl chloride[48] (0.39 g, 1.62 mmol) was then added to the flask, followed by the addition of an excess of Na_2CO_3 (1.1 g, 9.7 mmol). This heterogeneous mixture was allowed to stir at room temperature. After 16 h, solids were filtered off and washed with excess MeCN (30 mL). The filtrate was then evaporated under vacuum to yield a crude product, which was subjected to silica gel column chromatography eluting with a DCM/MeOH solvent mixture (gradient from 100:0 to 92:8). Fractions containing the desired product were combined and concentrated under vacuum to yield **15** as a yellow sticky solid (0.34 g, 60%). R_f 0.4 (DCM/MeOH, 90:10); $[\alpha]_D^{20} = +4.53$ (*c* 0.19, MeOH); FT-IR (cast film) $\hat{v}$ max = 3328, 3113, 2929, 1664, 1609, 1530, 1486, 1459, 1350, 1269, 1241 cm^{-1}. ^{1}H NMR (700 MHz, D$_2$O): δ 8.71 (dd, *J* = 6.8, 2.4 Hz, 1H), 8.30 (dq, *J* = 8.9, 2.7 Hz, 1H), 7.71−7.64 (m, 1H), 4.00 (t, *J* = 7.8 Hz, 1H), 3.86 (dddd, *J* = 8.2, 4.5, 2.6, 1.0 Hz, 1H), 3.82−3.78 (m, 1H), 3.78−3.75 (m, 1H), 3.73 (d, *J* = 2.8 Hz, 1H), 3.70 (dd, *J* = 12.5, 2.7 Hz, 1H), 3.61 (dd, *J* = 12.6, 5.0 Hz, 1H), 3.52 (dd, *J* = 12.5, 4.5 Hz, 1H), 4 exchangeable protons were not detected in D$_2$O solution. ^{13}C NMR (176 MHz, CD$_3$OD): δ 158.57 (d, J_{C-F} = 268.7 Hz), 140.5 (d, J_{C-F} = 3.9 Hz), 138.5, 135.4 (d, J_{C-F} = 10.3 Hz), 126.7, 120.5 (d, J_{C-F} = 22.2 Hz), 4.6, 83.0, 76.7, 62.6, 62.4, 61.7. HRMS (ESI) calcd for C$_{12}$H$_{14}$FN$_2$O$_8$S [M − H]$^-$ 365.0460; found 365.0459. HPLC purity >99%.

3-Deoxy-3-[*N*-(1-(4-fluoro-3-(trifluoromethyl)phenyl)-carbamothioyl)amino]-2,5-anhydro-D-mannitol (17). In a one-neck 50 mL round-bottom flask, maintained under N_2 atmosphere, amine **7** (0.11 g, 0.67 mmol) was dissolved in MeOH (15 mL). 4-Fluorophenyl-3-(trifluoromethyl)phenyl isothiocyanate (0.22 g, 1.0 mmol) was added to the flask, and vigorous stirring of the homogeneous mixture was continued at room temperature for 15 h. MeOH was removed under reduced pressure, and the crude compound was purified via silica gel column chromatography using a DCM/MeOH solvent mixture (gradient from 100:0 to 95:5). Fractions containing the desired product were combined and concentrated under vacuum to provide **17** as a brown oil (0.14 g, 54%). R_f 0.31 (DCM/MeOH, 90:10); $[\alpha]_D^{20} = +4.4$ (*c* 0.20, MeOH); IR (cast film) $\hat{v}$ max = 3298, 3067, 2927, 1707, 1628, 1545, 1507, 1436, 1327, 1269, 1235, 1166 cm^{-1}. ^{1}H NMR (400 MHz, CD$_3$OD): δ 7.80 (dd, *J* = 6.5, 2.7 Hz, 1H), 7.65 (dt, *J* = 7.5, 3.4 Hz, 1H), 7.28 (t, *J* = 9.6 Hz, 1H), 4.17 (t, *J* = 5.9 Hz, 1H), 3.96−3.93 (m, 1H), 3.93−3.89 (m, 1H), 3.80 (dd, *J* = 12.0, 3.5 Hz, 1H), 3.77−3.74 (m, 1H) 3.72 (d, *J* = 2.9 Hz, 1H), 3.63 (d, *J* = 4.4 Hz, 1H), 3.60 (d, *J* = 4.3 Hz, 1H), 5 exchangeable protons were not detected in CD$_3$OD solution. ^{13}C NMR (176 MHz, CD$_3$OD): δ 182.1, 156.6 (d, J_{C-F} = 253.4 Hz), 135.3, 130.1 (d, J_{C-F} = 6.8 Hz), 122.8, 122.4 (q, J_{C-F} = 271.3 Hz), 119.1 (d, J_{C-F} = 26.4 Hz), 116.8 (d, J_{C-F} = 28.0 Hz), 84.6, 83.6, 76.2, 62.9, 62.2, 61.6. HRMS (ESI) calcd for C$_{14}$H$_{16}$F$_4$N$_2$O$_4$SNa [M + Na]$^+$ 407.0659; found 407.0659. HPLC purity >90%.

General Procedure to Synthesize 18−21. A flask maintained under N_2 atmosphere was charged with amine **7** (0.13 g, 1.2 mmol) and freshly distilled DMF (20 mL). At room temperature, an excess of $NaHCO_3$ (5.3 g, 6.3 mmol) was added to the reaction mixture, followed by the addition of the isocyanate derivative: for **18**, benzyl isocyanate (0.16 g, 1.2 mmol); for **19**, 4-fluorophenyl isocyanate (0.16 g, 1.2 mmol); for **20**, 4-fluorophenyl-3-(trifluoromethyl)phenyl isocyanate (0.24 g, 1.2 mmol); for **21**, 4-fluorophenyl-3-nitrophenyl isocyanate (0.21 g, 1.2 mmol). The mixture was left to stir for 16 h before solids were filtered off and the filtrate was removed under reduced pressure. The resultant crude product was purified by subjecting to silica gel column chromatography eluted with a DCM/MeOH solvent mixture (gradient from 100:0 to 94:6 for **18**; 100:0 to 92:8 for **19**; 100:0 to 92:8 for **20**; 100:0 to 93:7 for **21**). Fractions

containing the desired product were combined and concentrated under vacuum to yield the pure compound.

3-Deoxy-3-[N-(1-(benzyl)carbamoyl)amino]-2,5-anhydro-D-mannitol (18). White sticky solid (0.20 g, 86%). R_f 0.45 (DCM/MeOH, 90:10); $[\alpha]_D^{20}$= +7.00 (c 0.10, MeOH); IR (cast film) 3329, 2923, 1648, 1567, 1453, 1315, 1056, 830, 701 cm^{-1}. ^{1}H NMR (600 MHz, CD$_3$OD): δ 7.33−7.26 (m, 4H), 7.24−7.20 (m, 1H), 4.32 (d, J_{AB} = 15.8 Hz, 1H), 4.30 (d, J_{AB} = 15.8 Hz, 1H), 4.01−3.98 (m, 2H), 3.82 (tt, J = 4.9, 2.9 Hz, 1H), 3.77 (ddd, J = 7.7, 5.4, 3.3 Hz, 1H), 3.73 (dd, J = 12.0, 3.0 Hz, 1H), 3.70 (dd, J = 12.0, 3.4 Hz, 1H), 3.65−3.62 (m, 1H), 3.62−3.59 (m, 1H), 5 exchangeable protons were not detected in CD$_3$OD solution. ^{13}C NMR (176 MHz, CD$_3$OD): δ 159.6, 139.6, 128.0, 126.8, 126.6, 83.5, 82.6, 75.9, 62.2, 61.6, 58.7, 43.3. HRMS (ESI) calcd for C$_{14}$H$_{20}$N$_2$O$_5$ [M + H]$^+$ 297.1445; found 297.1450. HPLC purity >97%.

3-Deoxy-3-[N-(1-(4-fluorophenyl)carbamoyl)amino]-2,5-anhydro-D-mannitol (19). White sticky solid (0.16 g, 66%). R_f 0.25 (DCM/MeOH, 90:10); $[\alpha]_D^{20}$= +7.87 (c 0.32, MeOH); IR (cast film) 3322, 2924, 2855, 1677, 1614, 1564, 1510, 1460, 1407, 1310, 1216, 1156 cm^{-1}. ^{1}H NMR (700 MHz, D$_2$O): δ 7.29 (dd, J = 8.9, 4.9 Hz, 2H), 7.13 (t, J = 8.9 Hz, 2H), 4.17 (t, J = 7.8 Hz, 1H), 4.15 (t, J = 7.3 Hz, 1H), 3.96 (ddd, J = 7.3, 5.0, 2.9 Hz, 1H), 3.93 (ddd, J = 8.2, 5.4, 2.9 Hz, 1H), 3.83−3.81 (m, 1H), 3.81−3.78 (m, 1H), 3.72 (dd, J = 5.3, 2.7 Hz, 1H), 3.70 (dd, J = 5.4, 2.7 Hz, 1H), 5 exchangeable protons were not detected in D$_2$O solution. ^{13}C NMR (176 MHz, CD$_3$OD): δ 160.6, 158.7 (d, J_{C-F} = 171.6 Hz), 136.8, 122.2 (d, J_{C-F} = 7.8 Hz), 116.1 (d, J_{C-F} = 22.7 Hz), 85.1, 84.1, 77.3, 63.7, 63.0, 60.0. HRMS (ESI) calcd for C$_{13}$H$_{17}$FN$_2$O$_5$Na [M + Na]$^+$ 323.1014; found 323.1013. HPLC purity >99%.

3-Deoxy-3-[N-(1-(4-fluoro-3-(trifluoromethyl)phenyl)-carbamoyl)amino]-2,5-anhydro-D-mannitol (20). White sticky solid (0.18 g, 61%). R_f 0.26 (DCM/MeOH, 90:10); $[\alpha]_D^{20}$= +13.44 (c 0.18, MeOH); IR (cast film) 3323, 2940, 2879, 1678, 1629, 1611, 1568, 1505, 1428, 1331, 1255, 1226, 1135 cm^{-1}. ^{1}H NMR (700 MHz, CD$_3$OD): δ 7.80 (dd, J = 6.3, 2.8 Hz, 1H), 7.56 (ddd, J = 9.1, 4.2, 3.0 Hz, 1H), 7.21 (t, J = 9.6 Hz, 1H), 4.11−4.08 (m, 1H), 4.08−4.05 (m, 1H), 3.87−3.85 (m, 1H), 3.85−3.83 (m, 1H), 3.77−3.75 (m, 1H), 3.75−3.72 (m, 1H), 3.67 (dd, J = 12.0, 5.6 Hz, 1H), 3.64 (dd, J = 11.9, 4.6 Hz, 1H), 5 exchangeable protons were not detected in CD$_3$OD solution. ^{13}C NMR (176 MHz, CD$_3$OD): δ 157.8, 156.1 (d, J_{C-F} = 249.4 Hz), 137.6, 125.4 (d, J_{C-F} = 7.8 Hz), 124.1 (q, J_{C-F} = 271.2 Hz), 118.9 (d, J_{C-F} = 13.2 Hz), 118.8 (d, J_{C-F} = 13.1 Hz), 118.1 (d, J_{C-F} = 21.8 Hz), 85.1, 84.1, 77.2, 63.7, 63.1, 59.9. HRMS (ESI) calcd for C$_{14}$H$_{15}$F$_4$N$_2$O$_5$ [M − H]$^-$ 367.0923; found 367.0918. HPLC purity >99%.

3-Deoxy-3-[N-(1-(4-fluoro-3-nitrophenyl)carbamoyl)amino]-2,5-anhydro-D-mannitol (21). Yellowish white sticky solid (0.15 g, 55%). R_f 0.25 (DCM/MeOH, 90:10); $[\alpha]_D^{20}$= +11.13 (c 0.23, MeOH); IR (cast film) 3326, 3072, 2933, 1686, 1608, 1564, 1540, 1501, 1406, 1351, 1221 cm^{-1}. ^{1}H NMR (600 MHz, CD$_3$OD): δ 8.26 (dd, J = 6.6, 2.8 Hz, 1H), 7.62 (ddd, J = 9.1, 3.8, 2.8 Hz, 1H), 7.30 (dd, J = 10.8, 9.1 Hz, 1H), 4.11−4.08 (m, 1H), 4.06 (d, J = 6.6 Hz, 1H), 3.86 (td, J = 4.0, 3.5, 2.3 Hz, 1H), 3.85−3.83 (m, 1H), 3.77−3.74 (m, 1H), 3.74−3.71 (m, 1H), 3.67 (dd, J = 12.0, 5.6 Hz, 1H), 3.63 (dd, J = 12.0, 4.6 Hz, 1H), 5 exchangeable protons were not detected in CD$_3$OD solution. ^{13}C NMR (176 MHz, CD$_3$OD): δ 157.5, 151.6 (d, J_{C-F} = 257.5 Hz), 138.4 (d, J_{C-F} = 15.2 Hz), 137.9, 126.5 (d, J_{C-F} = 8.8 Hz), 119.3 (d, J_{C-F} = 22.1 Hz), 116.2, 85.1, 84.1, 77.2, 63.7, 63.1, 59.9. HRMS (ESI) calcd for C$_{13}$H$_{16}$FN$_3$O$_7$Na [M + Na]$^+$ 368.0864; found 368.0864. HPLC purity >99%.

In Vitro Cell Experiments

Instruments. A Cytation5 BioTek fluorescence plate reader was used to measure the 6-NBDF fluorescence in EMT6 cells.

Buffer Solutions. Glucose-free Krebs−Ringer buffer solution (120 mM NaCl, 25 mM NaHCO$_3$, 4 mM KCl, 1.2 mM KH$_2$PO$_4$, 2.5 mM MgSO$_4$, 70 μM CaCl$_2$, pH 7.4) was used for studies with EMT6 cells. Cold phosphate-buffered saline (PBS) (137 mM NaCl, 2.7 mM KCl, 10 mM Na$_2$HPO$_4$, 2 mM KH$_2$PO$_4$) was used to wash the extracellular probes.

Cell Culture. Murine EMT6 mammary gland tumor cells were grown in a humidified 5% CO$_2$ incubator at 37 °C in Gibco DMEM/F-12 medium supplemented with 15 mM HEPES, L-glutamine, 10% fetal bovine serum (GIBCO 12483; Gibco, Gaithersburg, MD), and 1% penicillin/streptomycin with medium renewal every 2 to 3 days.

Preparation of Samples. Fructose is freely soluble in Krebs−Ringer buffer solution. For 2,5-AM derivatives, all the samples were initially dissolved in ≤0.1% DMSO and were diluted using Krebs−Ringer buffer according to the required concentration maintaining ≤0.1% DMSO.

Concentration-Dependent Uptake of 6-NBDF into EMT6 Cells. EMT6 cells were allowed to reach confluence in 12-well cell culture plates with medium renewal every 2 days. One hour before conducting the uptake study, the medium was removed, and the plates were washed twice with glucose-free Krebs−Ringer buffer solution, after which 1 mL of Krebs−Ringer buffer solution was added to each well. The plates were incubated at 37 °C for 1 h under this glucose-free condition. After 1 h of incubation, Krebs−Ringer buffer was removed from each well, and 500 μL of Krebs−Ringer buffer containing different concentrations of 6-NBDF (10^{-7}, 10^{-4}, 9×10^{-4}, 10^{-3} M) was incubated within each well for a specific period (30 min) in a CO$_2$ incubator at 37 °C. After incubation, the medium was aspirated, and each well was rinsed with 1 mL of ice-cold PBS buffer (1×3), and the plates were stirred for 3 min on a rotating rocker after each wash. After rinsing, 1 mL of PBS buffer was added to each well, and the fluorescence count was measured via a fluorescence plate reader. The net fluorescence value corresponding to a specific well was calculated by subtracting the background fluorescence value (autofluorescence of a well with EMT6 cells and PBS buffer was referred as background fluorescence).

Time-Dependent Uptake of 6-NBDF into EMT6 Cells. EMT6 cells were allowed to reach confluence in 12-well cell culture plates with medium renewal every 2 days. One hour before conducting the uptake study, the medium was removed and the plates were washed twice with glucose-free Krebs−Ringer buffer solution, after which 1 mL of Krebs−Ringer buffer solution was added to each well. The plates were incubated at 37 °C for 1 h under this glucose-free condition. After 1 h of incubation, Krebs−Ringer buffer was removed from each well and 500 μM of Krebs−Ringer buffer containing 350 μM 6-NBDF was incubated within each well for different periods (0, 10, 20, 30, 45, 60, 90, 120 min) in a CO$_2$ incubator at 37 °C. After incubation, the medium was aspirated, and each well was rinsed with 1 mL of ice-cold PBS buffer (1×3), and the plates were stirred for 3 min on a rotating rocker after each wash. After rinsing, 1 mL of PBS buffer was added to each well, and the fluorescence count was measured via a fluorescence plate reader. The net fluorescence value corresponding to a specific well was calculated by subtracting the background fluorescence value (autofluorescence of a well with EMT6 cells and PBS buffer was referred as background fluorescence).

General Procedure for In Vitro Inhibition of 6-NBDF Uptake into EMT6 Cells. EMT6 cells were allowed to reach confluence in 12-well cell culture plates with medium renewal every 2 days. One hour before conducting the uptake study, the medium was removed and the plates were washed twice with glucose-free Krebs−Ringer buffer solution, after which 1 mL of Krebs−Ringer buffer solution was added to each well. The plates were incubated at 37 °C for 1 h under this glucose-free condition. After 1 h of incubation, Krebs−Ringer buffer was removed from each well, and 500 μL of glucose-free Krebs−Ringer buffer containing 350 μM of 6-NBDF and increasing concentrations of the 2,5-AM derivatives **8−21** (10^{-5} to 10^{-3} M), fructose (10^{-4} to 3 M), cytochalasin B (10^{-7} to 10^{-5} M), quercetin (10^{-7} to 10^{-5} M), or MSNBA (10^{-7} to 10^{-4} M) or no compound (only buffer and cells) as a negative control for comparison (=100% uptake) was added within each well for 1 h. After incubation, the medium was aspirated, and each well was rinsed with 1 mL of ice-cold PBS buffer (1×3), and the plates were stirred for 3 min on a rotating rocker after each wash. After rinsing, 1 mL of PBS buffer was added to each well, and the fluorescence count was measured via a fluorescence plate reader. The net fluorescence value corresponding to a specific well was calculated after subtracting the background fluorescence

value (autofluorescence of a well with EMT6 cells and PBS buffer was referred as background fluorescence). Competitive inhibition assays were carried out three times using different batches of cells. Data were analyzed as percent of maximum uptake of 6-NBDF. Graphs were constructed using GraphPad Prism 5.0 (GraphPad Software, San Diego, CA, U.S.A.), and half-maximum inhibition concentrations (IC_{50}) were determined from the concentration−inhibition curves through graphical analysis.

■ ASSOCIATED CONTENT

ⓢ Supporting Information

The Supporting Information is available free of charge at https://pubs.acs.org/doi/10.1021/acsbiomedche-mau.2c00056.

^{1}H NMR, ^{13}C NMR spectra and LC MS chromatograms of the newly synthesized compounds (PDF)

■ AUTHOR INFORMATION

Corresponding Author

F. G. West − *Department of Chemistry, University of Alberta, Edmonton, AB T6G 2G2, Canada; Department of Oncology, University of Alberta—Cross Cancer Institute, Edmonton, AB T6G IZ2, Canada; Cancer Research Institute of Northern Alberta, University of Alberta, Edmonton, AB T6G 2E1, Canada;* ⓞ orcid.org/0000-0001-7419-2314; Email: fwest@ualberta.ca

Authors

Natasha Rana − *Department of Chemistry, University of Alberta, Edmonton, AB T6G 2G2, Canada; Department of Oncology, University of Alberta—Cross Cancer Institute, Edmonton, AB T6G IZ2, Canada; Cancer Research Institute of Northern Alberta, University of Alberta, Edmonton, AB T6G 2E1, Canada*

Marwa A. Aziz − *Department of Chemistry, University of Alberta, Edmonton, AB T6G 2G2, Canada; Department of Pharmaceutical Chemistry, Faculty of Pharmacy, Ain Shams University, Abassia, Cairo 11566, Egypt*

Rabah A. T. Serya − *Department of Pharmaceutical Chemistry, Faculty of Pharmacy, Ain Shams University, Abassia, Cairo 11566, Egypt*

Deena S. Lasheen − *Department of Pharmaceutical Chemistry, Faculty of Pharmacy, Ain Shams University, Abassia, Cairo 11566, Egypt*

Nermin Samir − *Department of Pharmaceutical Chemistry, Faculty of Pharmacy, Ain Shams University, Abassia, Cairo 11566, Egypt*

Frank Wuest − *Department of Chemistry, University of Alberta, Edmonton, AB T6G 2G2, Canada; Department of Oncology, University of Alberta—Cross Cancer Institute, Edmonton, AB T6G IZ2, Canada;* ⓞ orcid.org/0000-0002-6705-6450

Khaled A. M. Abouzid − *Department of Pharmaceutical Chemistry, Faculty of Pharmacy, Ain Shams University, Abassia, Cairo 11566, Egypt*

Complete contact information is available at:
https://pubs.acs.org/10.1021/acsbiomedchemau.2c00056

Author Contributions

The project was conceived by F.W. and F.G.W. F.G.W. supervised N.R. F.G.W., K.AM.A., R.A.T.S., D.S.L., and N.S. supervised M.A.A. Synthesis and *in vitro* experiments were designed and performed by N.R. and M.A.A. M.A.A. wrote the manuscript, with input from N.R. The manuscript was edited by F.G.W., K.AM.A., R.A.T.S., D.S.L., and N.S. with input from all authors. All authors have read and agreed to the published version of the manuscript.

Notes

The authors declare no competing financial interest.

■ ACKNOWLEDGMENTS

■ REFERENCES

(1) Dashty, M. A quick look at biochemistry: Carbohydrate metabolism. *Clin. Biochem.* **2013**, *46* (15), 1339−1352.

(2) Navale, A. M.; Paranjape, A. N. Glucose transporters: physiological and pathological roles. *Biophys. Rev.* **2016**, *8* (1), 5−9.

(3) Manolescu, A. R.; Witkowska, K.; Kinnaird, A.; Cessford, T.; Cheeseman, C. Facilitated Hexose Transporters: New Perspectives on Form and Function. *Physiology* **2007**, *22* (4), 234−240.

(4) Wood, I. S.; Trayhurn, P. Glucose transporters (GLUT and SGLT): expanded families of sugar transport proteins. *Br. J. Nutr.* **2003**, *89* (1), 3−9.

(5) Poulsen, S. B.; Fenton, R. A.; Rieg, T. Sodium-glucose cotransport. *Curr. Opin. Nephrol. Hypertens.* **2015**, *24* (5), 463−469.

(6) Thorens, B.; Mueckler, M. Glucose transporters in the 21st Century. *Am. J. Physiol. Endocrinol. Metab.* **2010**, *298* (2), E141−5.

(7) Mueckler, M.; Thorens, B. The SLC2 (GLUT) family of membrane transporters. *Mol. Aspects Med.* **2013**, *34* (2), 121−138.

(8) Douard, V.; Ferraris, R. P. Regulation of the fructose transporter GLUT5 in health and disease. *Am. J. Physiol. Endocrinol. Metab.* **2008**, *295* (2), E227−E237.

(9) Uldry, M.; Thorens, B. The SLC2 family of facilitated hexose and polyol transporters. *Pflugers Arch.* **2004**, *447* (5), 480−489.

(10) Long, W.; Cheeseman, C. Structure of, and functional insight into the GLUT family of membrane transporters. *Cell Health Cytoskelet.* **2015**, *7* (7), 167−183.

(11) Deng, D.; Yan, N. GLUT, SGLT, and SWEET: Structural and mechanistic investigations of the glucose transporters. *Protein Sci.* **2016**, *25* (3), 546−558.

(12) Holman, G. D. Structure, function and regulation of mammalian glucose transporters of the SLC2 family. *Pflügers Arch. - Eur. J. Physiol.* **2020**, *472* (9), 1155−1175.

(13) McQuade, D. T.; Plutschack, M. B.; Seeberger, P. H. Passive fructose transporters in disease: a molecular overview of their structural specificity. *Org. Biomol. Chem.* **2013**, *11* (30), 4909−4920.

(14) Kouidhi, S.; Berrhouma, R.; Rouissi, K.; Jarboui, S.; Clerget-Froidevaux, M.; Seugnet, I.; Bchir, F.; Demeneix, B.; Guissouma, H.; Elgaaied, A. Human subcutaneous adipose tissue Glut 4 mRNA expression in obesity and type 2 diabetes. *Acta Diabetol.* **2013**, *50* (2), 227−232.

(15) Camps, M.; Castelló, A.; Muñoz, P.; Monfar, M.; Testar, X.; Palacín, M.; Zorzano, A. Effect of diabetes and fasting on GLUT-4 (muscle/fat) glucose-transporter expression in insulin-sensitive tissues. Heterogeneous response in heart, red and white muscle. *Biochem. J.* **1992**, *282*, 765−772.

(16) Shepherd, P. R.; Kahn, B. B. Glucose transporters and insulin action–implications for insulin resistance and diabetes mellitus. *N. Engl. J. Med.* **1999**, *341* (4), 248−257.

(17) Douard, V.; Ferraris, R. P. The role of fructose transporters in diseases linked to excessive fructose intake. *J. Physiol.* **2013**, *591* (2), 401−414.

(18) Smith, T. A. Facilitative glucose transporter expression in human cancer tissue. *Br. J. Biomed. Sci.* **1999**, *56* (4), 285−292.

(19) Adekola, K.; Rosen, S. T.; Shanmugam, M. Glucose transporters in cancer metabolism. *Curr. Opin. Oncol.* **2012**, *24* (6), 650−654.

(20) Fan, X.; Liu, H.; Liu, M.; Wang, Y.; Qiu, L.; Cui, Y. Increased utilization of fructose has a positive effect on the development of breast cancer. *PeerJ* **2017**, *5*, e3804.

(21) Zamora-León, S. P.; Golde, D. W.; Concha, I. I.; Rivas, C. I.; Delgado-López, F.; Baselga, J.; Nualart, F.; Vera, J. C. Expression of the fructose transporter GLUT5 in human breast cancer. *Proc. Natl. Acad. Sci. U. S. A.* **1996**, *93* (5), 1847−1852.

(22) Godoy, A.; Ulloa, V.; Rodríguez, F.; Reinicke, K.; Yañez, A.; García, M.; Medina, R.; Carrasco, M.; Barberis, S.; Castro, T.; Martínez, F.; Koch, X.; Vera, J.; Poblete, M.; Figueroa, C.; Peruzzo, B.; Pérez, F.; Nualart, F. Differential subcellular distribution of glucose transporters GLUT1−6 and GLUT9 in human cancer: ultrastructural localization of GLUT1 and GLUT5 in breast tumor tissues. *J. Cell. Physiol.* **2006**, *207* (3), 614−627.

(23) Medina Villaamil, V.; Aparicio Gallego, G.; Valbuena Rubira, L.; García Campelo, R.; Valladares-Ayerbes, M.; Grande Pulido, E.; Victoria Bolós, M.; Santamarina Caínzos, I.; Antón Aparicio, L. Fructose transporter Glut5 expression in clear renal cell carcinoma. *Oncol. Rep.* **2011**, *25* (2), 315−323.

(24) Weng, Y.; Fan, X.; Bai, Y.; Wang, S.; Huang, H.; Yang, H.; Zhu, J.; Zhang, F. SLC2A5 promotes lung adenocarcinoma cell growth and metastasis by enhancing fructose utilization. *Cell Death Discovery* **2018**, *4* (1), 38.

(25) Chen, W.; Wang, Y.; Zhao, A.; Xia, L.; Xie, G.; Su, M.; Zhao, L.; Liu, J.; Qu, C.; Wei, R.; Rajani, C.; Ni, Y.; Cheng, Z.; Chen, Z.; Chen, S.; Jia, W. Enhanced Fructose Utilization Mediated by SLC2A5 Is a Unique Metabolic Feature of Acute Myeloid Leukemia with Therapeutic Potential. *Cancer Cell* **2016**, *30* (5), 779−791.

(26) Hamann, I.; Krys, D.; Glubrecht, D.; Bouvet, V.; Marshall, A.; Vos, L.; Mackey, J. R.; Wuest, M.; Wuest, F. Expression and function of hexose transporters GLUT1, GLUT2, and GLUT5 in breast cancer—effects of hypoxia. *FASEB J.* **2018**, *32* (9), 5104−5118.

(27) Yan, N. Structural advances for the major facilitator superfamily (MFS) transporters. *Trends Biochem. Sci.* **2013**, *38* (3), 151−159.

(28) Madej, M. G.; Sun, L.; Yan, N.; Kaback, H. R. Functional architecture of MFS D-glucose transporters. *Proc. Natl. Acad. Sci. U. S. A.* **2014**, *111* (7), E719−27.

(29) Nomura, N.; Verdon, G.; Kang, H. J.; Shimamura, T.; Nomura, Y.; Sonoda, Y.; Hussien, S. A.; Qureshi, A. A.; Coincon, M.; Sato, Y.; Abe, H.; Nakada-Nakura, Y.; Hino, T.; Arakawa, T.; Kusano-Arai, O.; Iwanari, H.; Murata, T.; Kobayashi, T.; Hamakubo, T.; Kasahara, M.; Iwata, S.; Drew, D. Structure and mechanism of the mammalian fructose transporter GLUT5. *Nature* **2015**, *526* (7573), 397−401.

(30) Deng, D.; Xu, C.; Sun, P.; Wu, J.; Yan, C.; Hu, M.; Yan, N. Crystal structure of the human glucose transporter GLUT1. *Nature* **2014**, *510* (7503), 121−125.

(31) Soueidan, O. M.; Scully, T. W.; Kaur, J.; Panigrahi, R.; Belovodskiy, A.; Do, V.; Matier, C. D.; Lemieux, M. J.; Wuest, F.; Cheeseman, C.; West, F. G. Fluorescent Hexose Conjugates Establish Stringent Stereochemical Requirement by GLUT5 for Recognition and Transport of Monosaccharides. *ACS Chem. Biol.* **2017**, *12* (4), 1087−1094.

(32) Tatibouët, A.; Yang, J.; Morin, C.; Holman, G. D. Synthesis and evaluation of fructose analogues as inhibitors of the D-fructose transporter GLUT5. *Bioorg. Med. Chem.* **2000**, *8* (7), 1825−1833.

(33) Tanasova, M.; Fedie, J. R. Molecular Tools for Facilitative Carbohydrate Transporters (Gluts). *Chembiochem* **2017**, *18* (18), 1774−1788.

(34) Yang, J.; Dowden, J.; Tatibouët, A.; Hatanaka, Y.; Holman, G. D. Development of high-affinity ligands and photoaffinity labels for the D-fructose transporter GLUT5. *Biochem. J.* **2002**, *367*, 533−539.

(35) Trayner, B. J.; Grant, T. N.; West, F. G.; Cheeseman, C. I. Synthesis and characterization of 6-deoxy-6-fluoro-D-fructose as a potential compound for imaging breast cancer with PET. *Bioorg. Med. Chem.* **2009**, *17* (15), 5488−5495.

(36) Levi, J.; Cheng, Z.; Gheysens, O.; Patel, M.; Chan, C.; Wang, Y.; Namavari, M.; Gambhir, S. Fluorescent fructose derivatives for imaging breast cancer cells. *Bioconjugate Chem.* **2007**, *18* (3), 628−634.

(37) Wuest, M.; Trayner, B. J.; Grant, T. N.; Jans, H. S.; Mercer, J. R.; Murray, D.; West, F. G.; McEwan, A. J.; Wuest, F.; Cheeseman, C. I. Radiopharmacological evaluation of 6-deoxy-6-[18F]fluoro-d-fructose as a radiotracer for PET imaging of GLUT5 in breast cancer. *Nucl. Med. Biol.* **2011**, *38* (4), 461−475.

(38) Kumar Kondapi, V. P.; Soueidan, O. M.; Cheeseman, C. I.; West, F. G. Tunable GLUT−Hexose Binding and Transport via Modulation of Hexose C-3 Hydrogen-Bonding Capabilities. *Chem. - A Eur. J.* **2017**, *23* (33), 8073−8081.

(39) Rana, N.; Aziz, M. A.; Oraby, A. K.; Wuest, M.; Dufour, J.; Abouzid, K. A.; Wuest, F.; West, F. G. Towards Selective Binding to the GLUT5 Transporter: Synthesis, Molecular Dynamics and In Vitro Evaluation of Novel C-3-Modified 2,5-Anhydro-D-mannitol Analogs. *Pharmaceutics* **2022**, *14* (4), 828.

(40) Hellwig, B.; Joost, H. G. Differentiation of erythrocyte-(GLUT1), liver-(GLUT2), and adipocyte-type (GLUT4) glucose transporters by binding of the inhibitory ligands cytochalasin B, forskolin, dipyridamole, and isobutylmethylxanthine. *Mol. Pharmacol.* **1991**, *40* (3), 383−389.

(41) Kapoor, K.; Finer-Moore, J. S.; Pedersen, B. P.; Caboni, L.; Waight, A.; Hillig, R. C.; Bringmann, P.; Heisler, I.; Müller, T.; Siebeneicher, H.; Stroud, R. M. Mechanism of inhibition of human glucose transporter GLUT1 is conserved between cytochalasin B and phenylalanine amides. *Proc. Natl. Acad. Sci. U. S. A.* **2016**, *113* (17), 4711−4716.

(42) Hamilton, K. E.; Rekman, J. F.; Gunnink, L. K.; Busscher, B. M.; Scott, J. L.; Tidball, A. M.; Stehouwer, N. R.; Johnecheck, G. N.; Looyenga, B. D.; Louters, L. L. Quercetin inhibits glucose transport by binding to an exofacial site on GLUT1. *Biochimie* **2018**, *151*, 107−114.

(43) Kwon, O.; Eck, P.; Chen, S.; Corpe, C.; Lee, J.; Kruhlak, M.; Levine, M. Inhibition of the intestinal glucose transporter GLUT2 by flavonoids. *FASEB J.* **2007**, *21* (2), 366−377.

(44) George Thompson, A. M.; Ursu, O.; Babkin, P.; Iancu, C. V.; Whang, A.; Oprea, T. I.; Choe, J.-y. Discovery of a specific inhibitor of human GLUT5 by virtual screening and in vitro transport evaluation. *Sci. Rep.* **2016**, *6* (1), 24240.

(45) Tripp, J.; Essl, C.; Iancu, C. V.; Boles, E.; Choe, J.; Oreb, M. Establishing a yeast-based screening system for discovery of human GLUT5 inhibitors and activators. *Sci. Rep.* **2017**, *7* (1), 6197.

(46) Kumar Kondapi, V. P.; Soueidan, O. M.; Hosseini, S. N.; Jabari, N.; West, F. G. Efficient and Easy Access to Optically Pure Tetrasubstituted Tetrahydrofurans via Stereoselective Opening of C2-Symmetric Epoxide and Aziridine Rings. *Eur. J. Org. Chem.* **2016**, *2016* (7), 1367−1379.

(47) Ren, C.; Wang, T.; Zhang, Y.; Peng, D.; Liu, X.; Wu, Q.; Liu, X.; Luo, S. Photoinduced Activation of Unactivated C(sp3)-H Bonds and Acylation Reactions. *ChemistrySelect* **2021**, *6* (10), 2523−2528.

(48) Lawhorn, B.; Philp, J.; Zhao, Y.; Louer, C.; Hammond, M.; Cheung, M.; Fries, H.; Graves, A.; Shewchuk, L.; Wang, L.; Cottom, J.; Qi, H.; Zhao, H.; Totoritis, R.; Zhang, G.; Schwartz, B.; Li, H.; Sweitzer, S.; Holt, D.; Gatto, G.; Kallander, L. Identification of Purines and 7-Deazapurines as Potent and Selective Type I Inhibitors of Troponin I-Interacting Kinase (TNNI3K). *J. Med. Chem.* **2015**, *58* (18), 7431−7448.

(49) Wuest, M.; Hamann, I.; Bouvet, V.; Glubrecht, D.; Marshall, A.; Trayner, B.; Soueidan, O. M.; Krys, D.; Wagner, M.; Cheeseman, C.; West, F.; Wuest, F. Molecular Imaging of GLUT1 and GLUT5 in Breast Cancer: A Multitracer Positron Emission Tomography Imaging Study in Mice. *Mol. Pharmacol.* **2018**, *93* (2), 79−89.

(50) As with any fluorescence-based assay, a HTS using 6-NBDF would need to counter screen for potential confounding results arising from intrinsic fluorescence of some members of the screening library.

(51) Simoneau, B. Preparation of non-nucleoside reverse transcriptase inhibitors. WO 2001096338 A1, 2001.

(52) Shackelford, S. A.; Anderson, M. B.; Christie, L. C.; Goetzen, T.; Guzman, M. C.; Hananel, M. A.; Kornreich, W. D.; Li, H.; Pathak, V. P.; Rabinovich, A. K.; Rajapakse, R. J.; Truesdale, L. K.; Tsank, S. M.; Vazir, H. N. Electrophilic Tetraalkylammonium Nitrate Nitration. II. Improved Anhydrous Aromatic and Heteroaromatic Mononitration with Tetramethylammonium Nitrate and Triflic Anhydride, Including Selected Microwave Examples. *J. Org. Chem.* **2003**, *68* (2), 267−275.